ORNL/TM-2023/2949

On-line Measurement of Hydrogen Gas using Raman Spectroscopy for Process Gas Systems

Kathryn M. Peruski
Breanna K. Vestal
Matt Vick
Chase Cobble
Katherine R. Johnson
Joanna McFarlane

July 2023

OAK RIDGE
National Laboratory

ORNL IS MANAGED BY UT-BATTELLE LLC FOR THE US DEPARTMENT OF ENERGY

DOCUMENT AVAILABILITY

Reports produced after January 1, 1996, are generally available free via OSTI.GOV.

Website www.osti.gov

Reports produced before January 1, 1996, may be purchased by members of the public from the following source:

National Technical Information Service
5285 Port Royal Road
Springfield, VA 22161
Telephone 703-605-6000 (1-800-553-6847)
TDD 703-487-4639
Fax 703-605-6900
E-mail info@ntis.gov
Website http://classic.ntis.gov/

Reports are available to US Department of Energy (DOE) employees, DOE contractors, Energy Technology Data Exchange representatives, and International Nuclear Information System representatives from the following source:

Office of Scientific and Technical Information
PO Box 62
Oak Ridge, TN 37831
Telephone 865-576-8401
Fax 865-576-5728
E-mail reports@osti.gov
Website https://www.osti.gov/

This report was prepared as an account of work sponsored by an agency of the United States Government. Neither the United States Government nor any agency thereof, nor any of their employees, makes any warranty, express or implied, or assumes any legal liability or responsibility for the accuracy, completeness, or usefulness of any information, apparatus, product, or process disclosed, or represents that its use would not infringe privately owned rights. Reference herein to any specific commercial product, process, or service by trade name, trademark, manufacturer, or otherwise, does not necessarily constitute or imply its endorsement, recommendation, or favoring by the United States Government or any agency thereof. The views and opinions of authors expressed herein do not necessarily state or reflect those of the United States Government or any agency thereof.

ORNL/TM-2023/2949

Nuclear Energy and Fuel Cycle Division

ON-LINE MEASUREMENT OF HYDROGEN GAS USING RAMAN SPECTROSCOPY FOR PROCESS GAS SYSTEMS

Kathryn M. Peruski
Breanna K. Vestal
Matt Vick
Chase Cobble
Katherine R. Johnson
Joanna McFarlane

July 2023

Prepared by
OAK RIDGE NATIONAL LABORATORY
Oak Ridge, TN 37831
managed by
UT-BATTELLE LLC
for the
US DEPARTMENT OF ENERGY
under contract DE-AC05-00OR22725

CONTENTS

LIST OF FIGURES

ABSTRACT

Advanced reprocessing schemes such as the Zircex process are important for continued development of the nuclear fuel cycle. The hydrochlorination reaction of the Zircex process flow sheet for metallic fuels has a known off-gas stream of $H_2(g)$ and HCl. The flow sheet can be simplified through HCl recycling, which requires detection and quantification of any residual $H_2(g)$ for safety and purity. In this work, commercially available Raman spectroscopy was applied for low-level, on-line detection of $H_2(g)$ in process gas streams, and parameters were adjusted to optimize the $H_2(g)$ Raman signal. Increasing the number of scans and exposure time in the spectrometer increased the signal-to-noise ratio of the $H_2(g)$ Raman signal, while the gas flow rate was optimized at 2.3 L/min. The limit of detection for $H_2(g)$ was estimated to be 2,100 ppm $H_2(g)$ in an $N_2(g)$ background. This scoping study for the application of Raman spectroscopy for on-line measurements of $H_2(g)$ shows that $H_2(g)$ can be detected at low levels (approximately 5% of the lower explosive limit (LEL)) in flowing gas streams.

1. INTRODUCTION

Advanced nuclear fuel reprocessing flow sheets can include many different chemical reactions that generate targeted products and unwanted by-products. One reprocessing technique under development is the Zircex process, which uses a solid-gas reaction first developed in the 1960s for metallic fuels.[1] The first part of the Zircex flow sheet utilizes gas-phase hydrochlorination to process metallic fuels, such as U-Zr fuel. The chemistry of the hydrochlorination reactions can be described with the following equations[2]:

$$Zr + 4HCl \rightarrow ZrCl_4 + 2H_2$$

$$U + 3HCl \rightarrow UCl_3 + 1.5H_2$$

One by-product of concern in the Zircex process is hydrogen gas ($H_2(g)$. Gens[2] estimates that 37.8 kg $H_2(g)$/100 kg of fuel is produced during hydrochlorination. Hydrogen is a concerning by-product because it is flammable and explosive at concentrations as low as 4% in air. The lower explosive limit (LEL) reported by the National Research Council is 4.1%.[3] The off-gas from hydrochlorination is predominantly water vapor, H_2, and HCl. Recycling the HCl from this off-gas stream can minimize waste and reduce the amount of feed HCl required for the process. Engineering flow sheets exist for separation of HCl from other by-products for recycle[4]; however, verification of complete $H_2(g)$ removal is essential. Given the known presence of $H_2(g)$ by-product in the Zircex flow sheet and the safety concerns associated with $H_2(g)$ buildup, detection and quantification of $H_2(g)$ are necessary in corrosive process gas streams such as an HCl recycle loop, ideally in an on-line measurement format.

The chemical properties of $H_2(g)$ and associated safety measures limit detection techniques. As a diatomic molecule with symmetric stretching, $H_2(g)$ is not detectable via infrared (IR) techniques, which are common for gas monitoring. Therefore, alternative sensing techniques must be considered, while also evaluating additional process gas concerns such as corrosive or O_2-free environments, which may limit materials of construction or applicable techniques. An evaluation of commercially available technologies identified that potential techniques for $H_2(g)$ detection include gas chromatography, mass spectrometry, Raman spectroscopy, thermal conductivity, electrochemical sensors, and various catalytic detectors such as Pt and Pd,[5] but many of these techniques are not compatible with corrosive or O_2-free gas streams or cannot be used in on-line monitoring.

Raman spectroscopy is a viable option for on-line $H_2(g)$ detection under corrosive conditions. The Raman spectra of $H_2(g)$ have been previously reported, with simulations for background-free (pure gas-phase)

Raman indicating that the $\nu_{0\text{-}1}$ vibrational transition occurs at 4,152 cm^{-1} and rotational peaks occur at 357, 592, 819, and 1,039 cm^{-1}.[6] However, these assigned peaks (Stokes lines) may vary as functions of gas pressure, temperature, and background gases.[7] Additionally, these peaks may be shifted in experimental measurements versus simulations. Experimental measurements of H_2(g) in air reported[8] a rotational peak at 588 cm^{-1} ,[8] and a vibrational peak at 4,155 cm^{-1} was reported in measurements of pure H_2(g).[9] Interferences from water in the system are not expected, as process gas streams are kept dry. However, in the case of any water or water vapor instrusion in the gas stream, the greatest impacts would be from the -OH stretching peaks, which would be in the range of 3000-3700 cm^{-1},[10] which would not overlap with H_2(g) peaks. Given that HCl will co-occur with H_2(g) in potential off-gas streams for Zircex, the potential interference of HCl(g) in Raman spectra must be considered as well. The Raman spectrum of HCl shows a series of peaks ranging from 2,700 to 2,900 cm^{-1}.[11-13] Even accounting for potential shift in the peaks due to different pressures, temperatures, or background matrices, the peaks associated with HCl(g) do not interfere with the Raman peaks associated with H_2(g), making the application of Raman spectroscopy appealing for the detection of H_2(g) in HCl(g) matrices.

Despite its inherent insensitivity, Raman spectroscopy has been used successfully for low-level H_2(g) detection. Specifically, recent studies on cavity-enhanced Raman spectroscopy (CERS) have reported detection limits of 460 ppm by volume[9] and as low as 24 ppb by volume[8]. The very low limit of detection (LOD) reported[8, 9] are due to the use of multiple mirrored reflection cycles in custom-built Raman cells. Commercially available Raman systems, which do not have multiple reflections within the cell, are expected to have higher LODs. These studies indicate that low-level measurements of H_2(g) are possible with a commercial instrument, especially with ongoing analytical advancements in Raman spectroscopy. However, these studies focused on closed-cell (static) measurements of H_2(g). For industrial applications, such as the Zircex process, on-line measurement within a gas stream is needed for off-gas verification.

The objective of this work is to measure H_2(g) on-line at low concentrations in potential process gas streams, which is achieved through optimization of H_2(g) peak intensity in Raman spectroscopy by varying settings, gas flow, and gas pressure. Ultimately, attempts to determine a LOD for H_2(g) are made. Within the broader objective of optimizing this technique, additional objectives included adjusting parameters of a commercially available Raman spectrometer such as exposure time, scan time, and varying gas flow rates through the on-line system.

2. MATERIALS AND METHODS

2.1 EXPERIMENTAL SETUP

Hydrogen gas detection was tested using a custom-built gas-handling manifold equipped with an in-line Raman cell. The manifold was built from 1/4 in. stainless steel tubing with two separate inlet gas streams: one for diluent gas and one for the H_2(g) stream. Ultrahigh-purity N_2(g) was used as the diluent gas, and a 4% H_2/96% N_2 gas mixture was the H_2(g) source. Gas flow was regulated using mass flow controllers. The two gas streams were mixed in-line before reaching the Raman spectrometer in the manifold system. The spectrometer was a Kaiser Raman Rxn2 analyzer, which has a 532 nm incident wavelength, 150–4,350 cm^{-1} spectral coverage, and a gas cell sample chamber.

2.2 TEST CONDITIONS

The H_2(g) flow and detection setup were used to optimize the spectrometer settings and gas flow to determine LODs for H_2(g) in Raman. The general operating procedure for testing included a 24 h warm-up time for the spectrometer before use, a 10 min purge of the manifold with the dry N_2(g) stream, and equilibration of the manifold for 5 min at the test conditions prior to measurements.

2.2.1 Test 1: Spectrometer Scan Number

The on-line Raman cell was tested with scan numbers ranging from 1 to 10 to assess the effect on H_2(g) signal response. The number of scans refers to the number of measurements the spectrometer collects for a given acquisition. The final spectrum is an average of all collected spectra. Tests included 1, 3, 5, and 10 scans for comparison, with all other parameters held constant. For each test, 15 psi of 4% H_2/96% N_2 (g) was flowing at a rate of 1.6 L/min (LPM) with no additional N_2(g) diluent. Scans were each conducted with a 1 min exposure time.

2.2.2 Test 2: Spectrometer Exposure Time

The on-line Raman cell was tested with measurement exposure times ranging from 1 to 15 min to assess the effect on H_2(g) signal response. The exposure time refers to the time the detector is exposed to the Raman signal for a given acquisition. Tests included 1, 3, 5, and 15 min exposure time for comparison, with all other parameters held constant. For each test, 15 psi of 4% H_2/96% N_2(g) was flowing at a rate of 1.6 LPM with no additional N_2(g) diluent. One scan was conducted for each exposure time.

2.2.3 Test 3: Gas Flow Rate

The on-line Raman cell was tested under varying gas flow rates to assess the effect on H_2(g) signal response. Tests included the following flow rates: static (no flow), 0.9, 1.6, 2.3, 5.4, and 9.9 LPM. For each test, 20 psi of 4% H_2/96% N_2(g) was used with no additional N_2(g) diluent. Measurements were performed with one scan at a 5 min exposure time.

2.2.4 Test 4: Limit of Detection

To determine the H_2(g) Raman response to varying concentrations of H_2(g), manifold testing was performed by blending 4% H_2/96% N_2(g) with N_2(g) diluent gas in different relative proportions. The combined flow rate of the system was held constant at 5 LPM, and each test included 3 scans, each with a 10 min exposure time. The concentrations of H_2(g) tested were 40,000, 24,000, 17,000, 10,000, 8,100, 4,000, 2,100, and 775 ppm.

3. RESULTS AND DISCUSSION

The rotational and vibrational Raman lines for H_2(g) (4%) in N_2(g) are shown in Figure 1. S_1 and S_3 correspond to the rotational Raman bands of the ortho-hydrogen, and Q_1 and Q_3 correspond to the vibrational Raman bands of the ortho-hydrogen. S_0 and S_2 correspond to the rotational Raman bands of para-hydrogen, and Q_2 corresponds to the vibrational Raman bands of para-hydrogen.[14] Note that in these spectra, $S_0(1)$ and $Q_1(1)$ are prominent, which is consistent with reported spectra for H_2(g). Additional peaks present in Figure 1 are due to N_2(g) or other backgrounds.

3.1 OPTIMIZATION OF SPECTROMETER SETTINGS

Scan number and exposure time in the Raman spectrometer are both key drivers of signal intensity for H_2(g) detection. Increasing the exposure time from 1 to 15 min in the spectrometer results in relative increases in intensity of the H_2(g) peaks at 588 cm^{-1} and 4,157 cm^{-1} (**Error! Reference source not found.**), and increasing the scan number from 1 to 10 total scans increases the relative intensity of H_2(g) peaks at 588 cm^{-1} and 4,157 cm^{-1} as well (**Error! Reference source not found.**). Because of the high-energy laser excitation source, increased scan number and exposure time also produce a significant fluorescence baseline.[15]

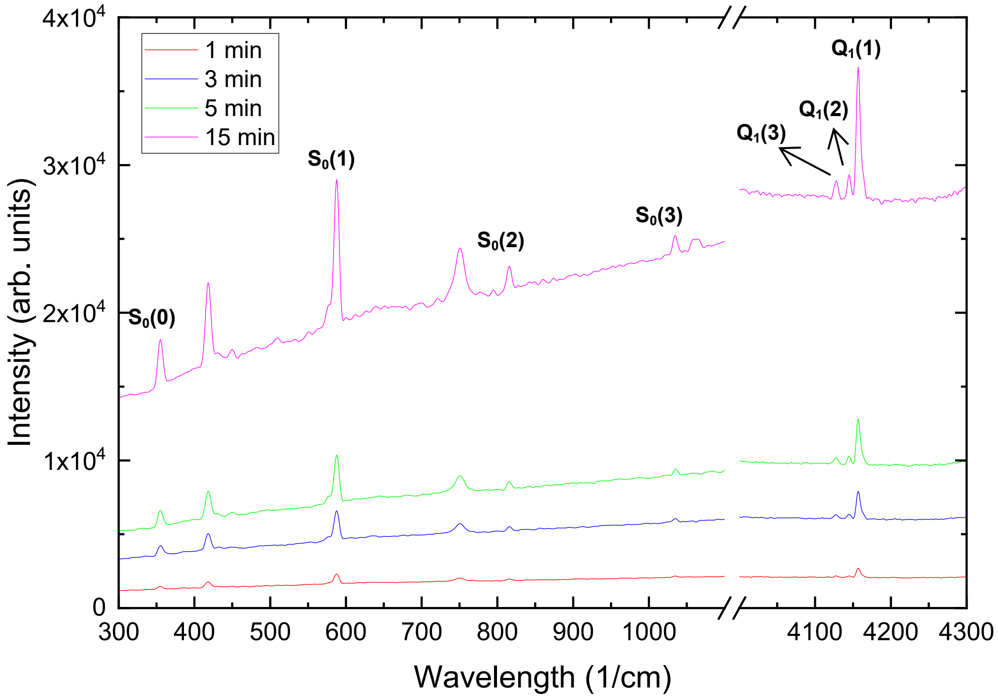

Figure 1. Raman spectra of 4% H_2(g) flowing at 1.6 LPM as as a function of exposure time at 300–1,100 cm^{-1} and 4,000–4,300 cm^{-1}. The characteristic Raman peak for N_2(g) (~2,330 cm^{-1}) is omitted for clarity.

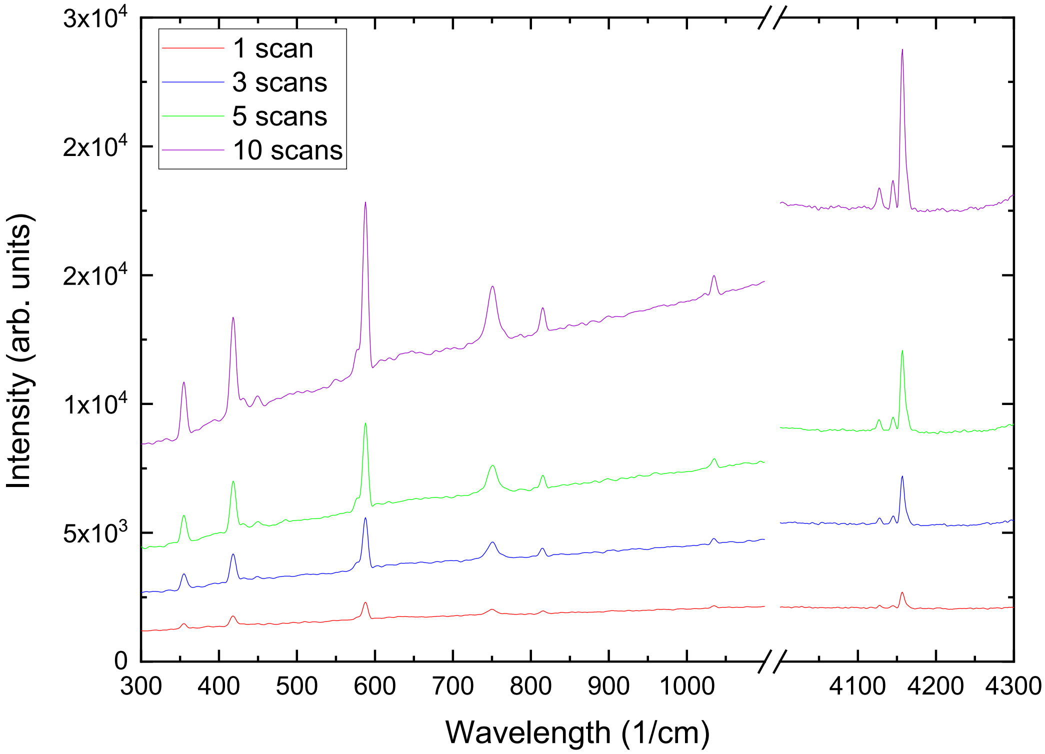

Figure 2. Raman spectra of 4% H_2(g) flowing at 1.6 LPM as a function of scan number at 300–1,100 cm^{-1} and 4,000–4,300 cm^{-1}. The characteristic Raman peak for N_2(g) (~2,330 cm^{-1}) is omitted for clarity.

Quantitative evaluation of peak area and peak height variation from changing scan number and exposure time indicate that optimum measurement settings are when scan number and exposure time are maximized. Peak area and height increase by approximately an order of magnitude when exposure time is increased from 1 to 15 min (Figure A-1). Similarly, peak height and area increase by a factor of approximately 5 when scan number is increased from 1 to 10 (Figure A-2). The maximized peak height and peak area at longer exposure times and higher scan numbers can enable measurement of lower concentrations of $H_2(g)$.

3.2 OPTIMIZATION OF GAS FLOW RATE

The flow rate of gas through the Raman flow cell alters the peak height and peak area of $H_2(g)$ peaks in the Raman spectrum, with maximum peak height and area achieved at 2.3 LPM. Graphically comparing the Raman spectra across 0–10 LPM, it is difficult to ascertain how flow rate changes the peak area and peak height (**Error! Reference source not found.**). However, the background of the spectra decreases at increasing flow rates, which yields a better signal-to-noise ratio. Quantitative analysis of the peak areas and heights under changing flow rates shows that peak areas and heights are maximized at 2.3 LPM. The peak area and height increase by 15%–30% increase from static conditions to 2.3 LPM, then decrease at higher flow rates (Figure 4).

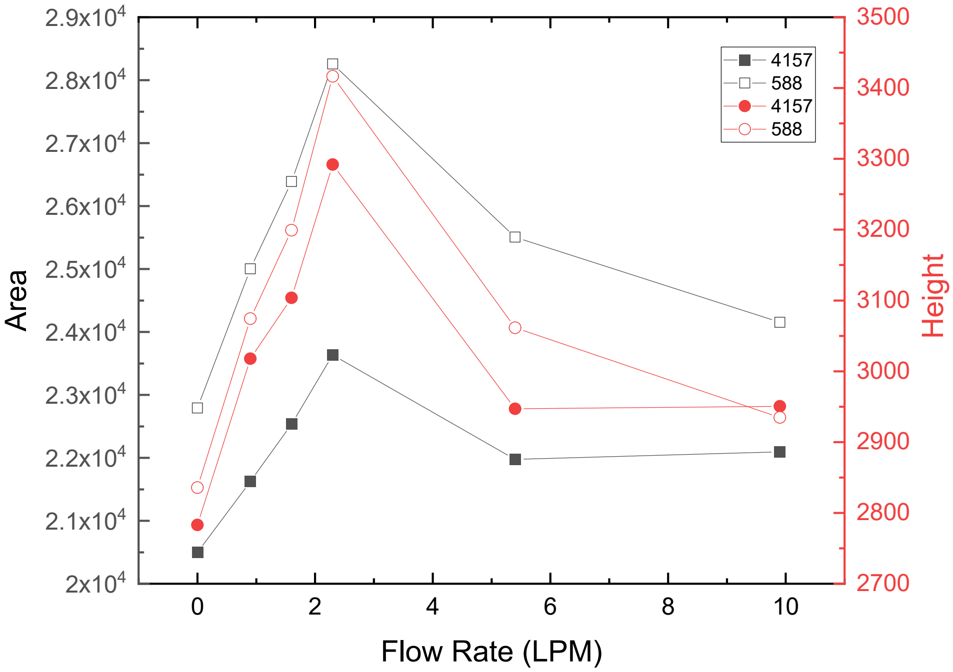

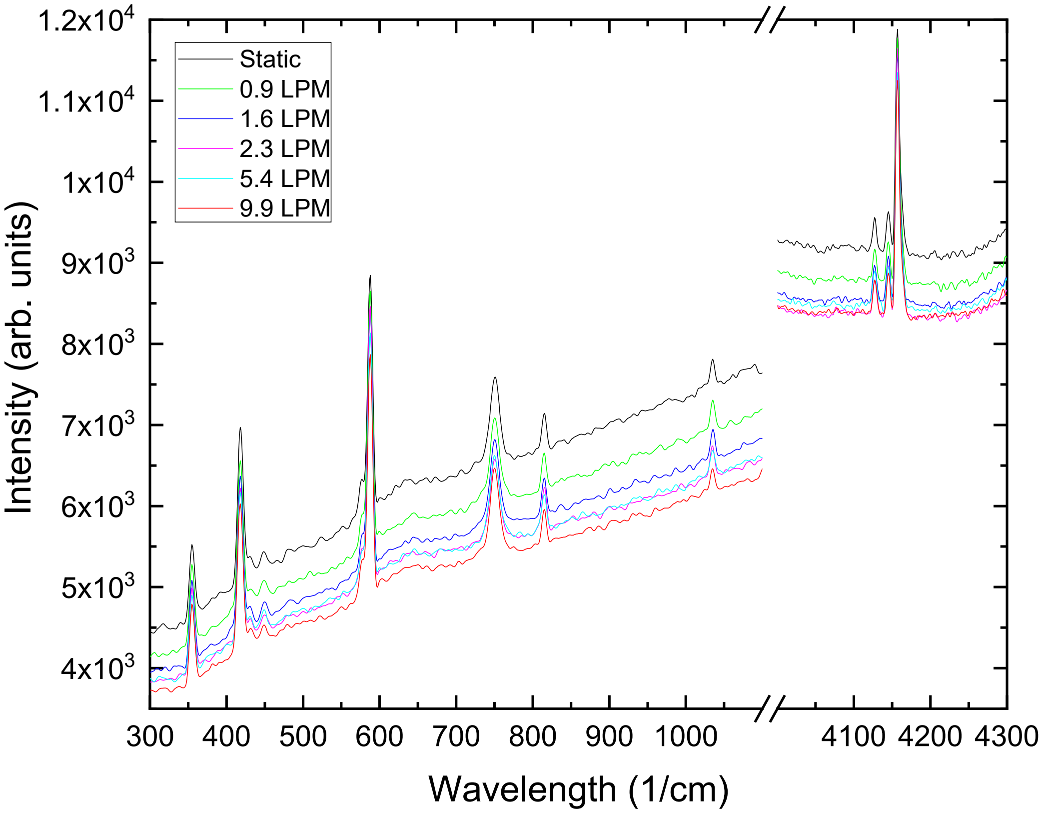

Figure 3. Raman spectra of 4% H_2(g) as functions of gas flow rate at 300–1,100 cm^{-1} and 4,000–4,300 cm^{-1}. The characteristic Raman peak for N_2(g) (~2,330 cm^{-1}) is omitted for clarity.

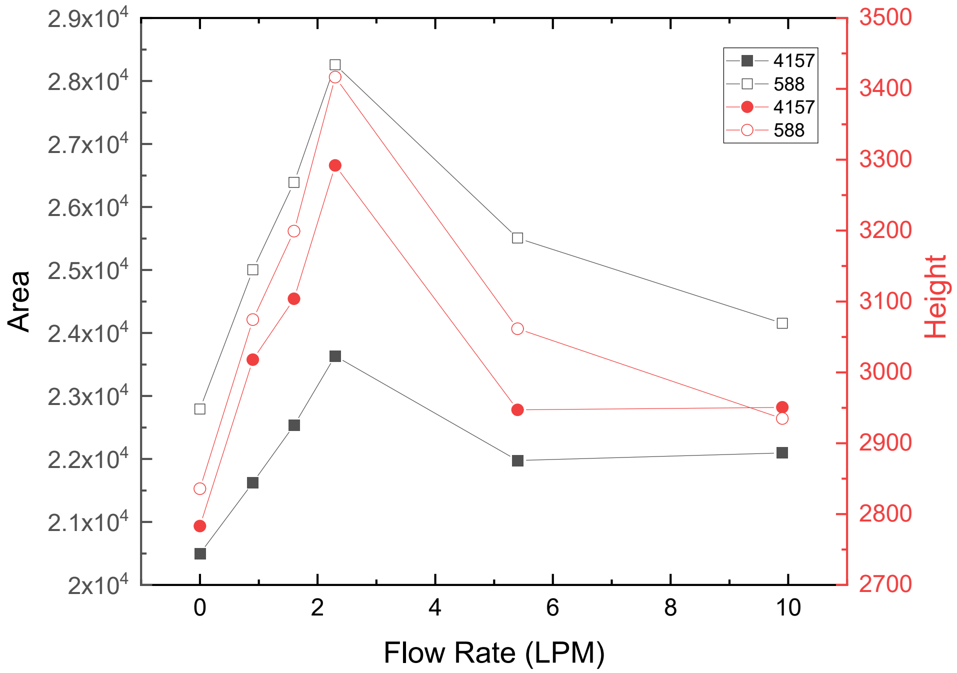

Figure 4. Peak area (black) and height (red) of Raman spectra of 4% H_2(g) at flow rates ranging from 0 to 10 LPM. In the key, 4157 and 588 refer to the wavelengths of the Raman peak (cm^{-1}) used to calculate area or height.

3.3 LIMIT OF DETECTION EVALUTAION

Raman spectral measurements of H_2(g) in flowing gas reveal that that detection is possible at an order of magnitude below the H_2(g) LEL. Positive measurement of H_2(g) was achieved at concentrations as low as 2,100 ppm in a flowing gas stream (Plots of peak area and height of the 4157 cm^{-1} Raman peak versus concentration indicate that both area and height vary linearly with H_2(g) concentration in the gas stream (Figure 6), suggesting that calibration curves could be developed for quantitative determination of H_2(g) in process gas streams. For peak area, the data can be fit linearly in OriginPro with adjusted R^2 of 0.997 according to the following equation:

$$H_2\ concentration\ (ppm) = (3.85 \times Peak\ Area) - 2967.80$$

Similarly, the peak height can be fit linearly in OriginPro with an adjusted R^2 of 0.997 according to the following equation:

$$H_2\ concentration\ (ppm) = (0.55 \times Peak\ Area) - 577.87$$

Although these calibration curves were determined for this specific experimental apparatus, the linearity of the data indicates that similar responses could be anticipated for a dedicated Raman system on the hydrochlorination off-gas. Greater sensitivity may be achieved by increasing the number of scans averaged to improve the signal-to-noise ratio, but doing so will reduce time resolution.

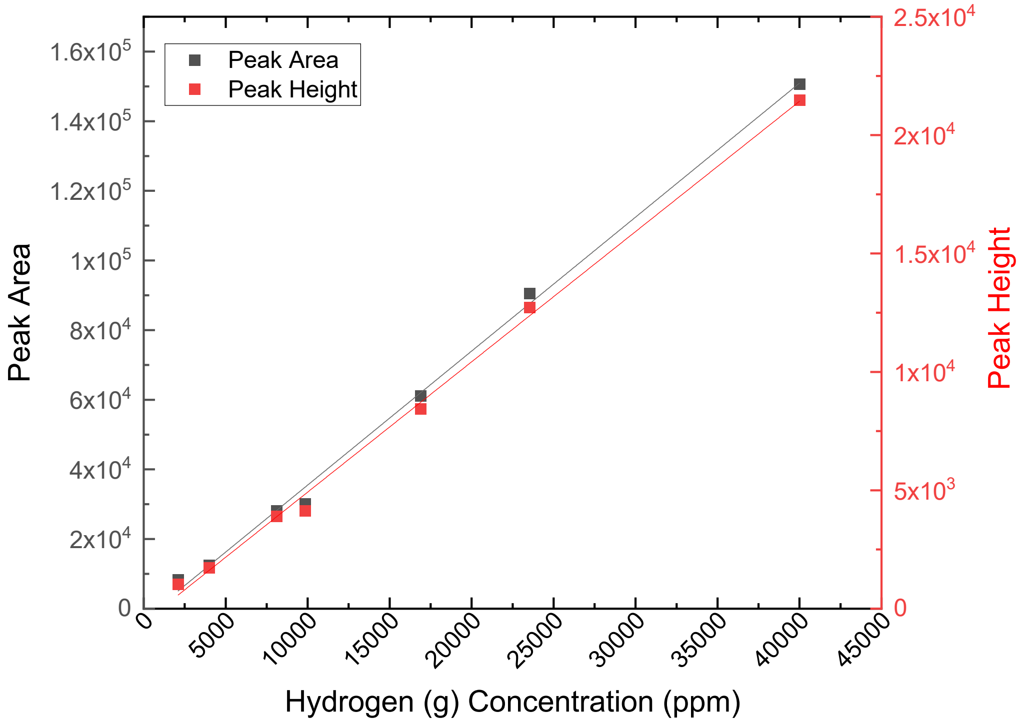

). Measurement of $H_2(g)$ at 775 ppm was attempted, but no peaks were observed in the spectrum.

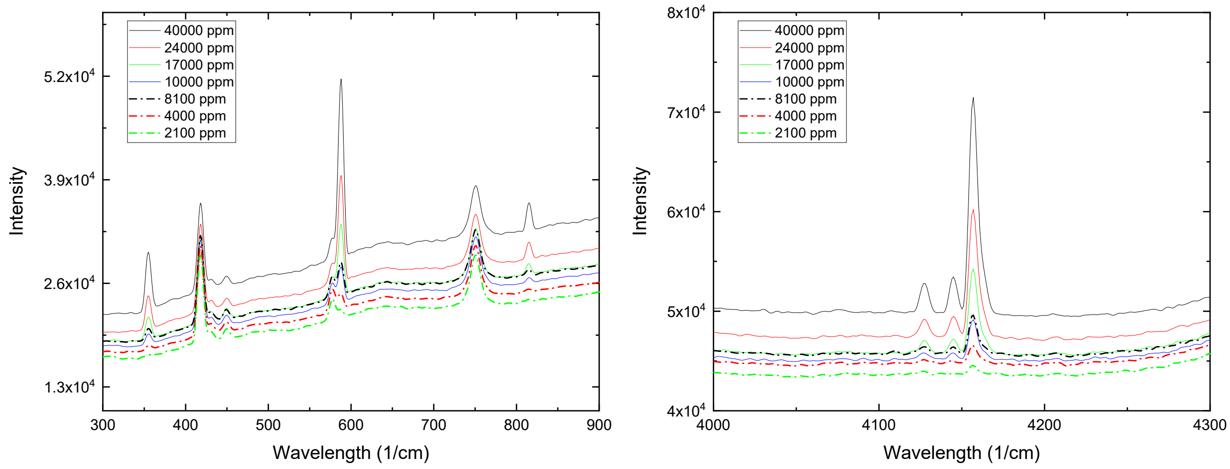

Figure 5. Raman spectra of $H_2(g)$ at concentrations of 2,100–40,000 ppm at 300–900 cm^{-1} (left) and 4,000–4,300 cm^{-1} (right).

Plots of peak area and height of the 4157 cm^{-1} Raman peak versus concentration indicate that both area and height vary linearly with $H_2(g)$ concentration in the gas stream (Figure 6), suggesting that calibration curves could be developed for quantitative determination of $H_2(g)$ in process gas streams. For peak area, the data can be fit linearly in OriginPro with adjusted R^2 of 0.997 according to the following equation:

$$H_2\ concentration\ (ppm) = (3.85 \times Peak\ Area) - 2967.80$$

Similarly, the peak height can be fit linearly in OriginPro with an adjusted R^2 of 0.997 according to the following equation:

$$H_2\ concentration\ (ppm) = (0.55 \times Peak\ Area) - 577.87$$

Although these calibration curves were determined for this specific experimental apparatus, the linearity of the data indicates that similar responses could be anticipated for a dedicated Raman system on the hydrochlorination off-gas. Greater sensitivity may be achieved by increasing the number of scans averaged to improve the signal-to-noise ratio, but doing so will reduce time resolution.

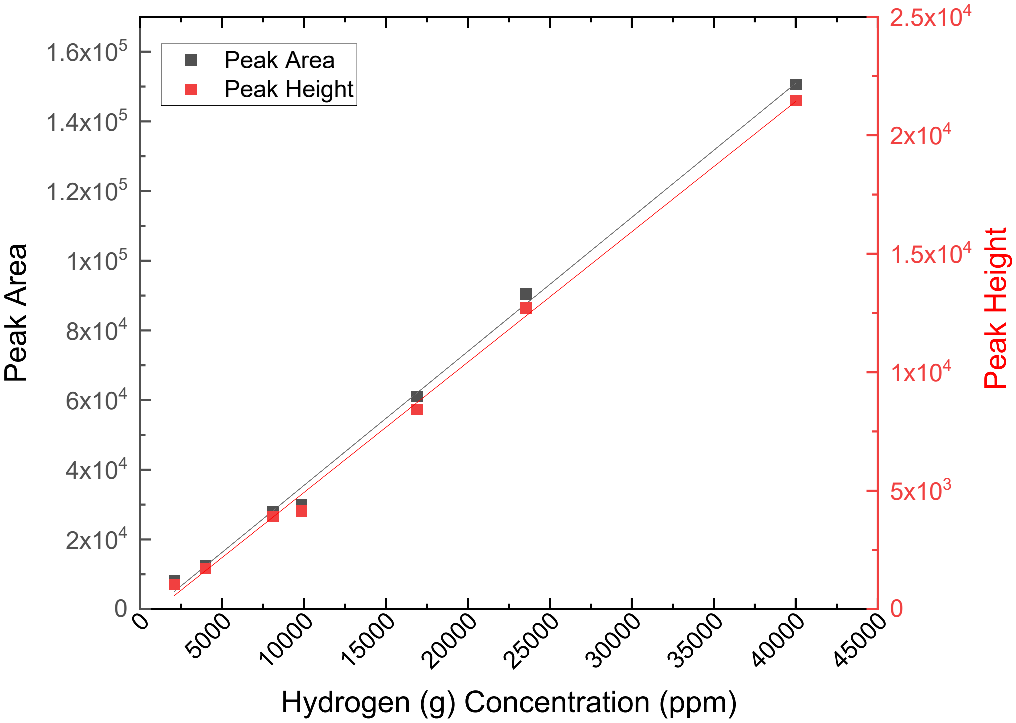

Figure 6. Peak area and height of the 4157 cm^{-1} Raman peak as functions of H_2(g) concentration in the gas stream.

4. CONCLUSIONS

Evaluation of Raman spectroscopy as a potential technique for on-line, low-level H_2(g) detection in process gas streams indicated the technique has potential utility. Laboratory testing was performed in a manifold to optimize H_2(g) signal in Raman spectra through variation in spectrometer settings, gas flow, and gas pressure and to determine the LOD for H_2(g). Increasing scan number and exposure time in the spectrometer increased the intensity of the H_2(g) Raman signal, as evidenced by increasing peak area and height. Increasing gas flow rates in the Raman cell did not produce a linear response in peak height and area; rather, peak height and area were maximized at 2.3 LPM. Very high flow rates (>9 LPM) and static conditions in the Raman cell produced the lowest intensity for H_2(g). Using a combination of parameters from the optimization tests, the LOD for H_2(g) was found to be approximately 2,100 ppm H_2(g) in an N_2(g) atmosphere. Overall, this work serves as a scoping study for the application of Raman spectroscopy for on-line measurements of flowing H_2(g) in process gas streams and shows that H_2(g) can be detected at low levels (approximately 5% of the LEL). To further develop this H_2(g) detection capability, additional investigations of the application of Raman for process gas streams, particularly corrosive gas streams, are necessary.

5. ACKNOWLEDGEMENTS

This work was supported by the US Department of Energy, Office of Nuclear Fuel Cycle and Supply Chain, Material Recovery and Waste Form Development Campaign (NE-43).

6. REFERENCES

1. Mcfarlane, J.; Braatz, A. D.; Birdwell Jr, J. F.; Bruffey, S.; Del Cul, G.; Greaney, A.; Hunt, R. D.; Ngelale, R.; Taylor, P. A.; Walker, T. In *Hydrochlorination at 200 C relevant to the removal of cladding from spent nuclear fuel*, American Nuclear Society, June 2021; Oak Ridge National Lab.(ORNL), Oak Ridge, TN (United States): 2021; pp 100-102.
2. Gens, T., *New Laboratory Developments in the Zircex Process*. Oak Ridge National Laboratory: 1961.
3. Council, N. R., *Emergency and Continuous Exposure Guidance Levels for Selected Submarine Contaminants: Volume 2*. National Academies Press: 2008; Vol. 2.
4. Gens, T. *Laboratory Development of a Combined Chloride Volatility-Aqueous Processing Method for Uranium-Zirconium Nuclear Fuels*; Oak Ridge National Lab., Tenn.: 1963.
5. Vestal, B.; Peruski, K. M.; McFarlane, J. *Commercially available hydrogen detection systems for corrosive, oxygen-free gas streams: A technical summary*; Oak Ridge National Laboratory: June 2023, 2023.
6. Odhner, J.; Romanov, D.; Levis, R. In *Filament-based stimulated Raman spectroscopy*, Nonlinear Frequency Generation and Conversion: Materials, Devices, and Applications IX, SPIE: 2010; pp 151-159.
7. Lallemand, P.; Simova, P., Stimulated Raman spectroscopy in hydrogen gas. *Journal of Molecular Spectroscopy* **1968,** *26* (2), 262-276.
8. Wang, P.; Chen, W.; Wang, J.; Zhou, F.; Hu, J.; Zhang, Z.; Wan, F., Hazardous gas detection by cavity-enhanced raman spectroscopy for environmental safety monitoring. *Analytical Chemistry* **2021,** *93* (46), 15474-15481.
9. Salter, R.; Chu, J.; Hippler, M., Cavity-enhanced Raman spectroscopy with optical feedback cw diode lasers for gas phase analysis and spectroscopy. *Analyst* **2012,** *137* (20), 4669-4676.
10. Carey, D. M.; Korenowski, G. M., Measurement of the Raman spectrum of liquid water. *The Journal of Chemical Physics* **1998,** *108* (7), 2669-2675.
11. Perchard, J.; Maillard, D.; Schriver, A.; Girardet, C., Structures of HCl and HBr polymers in nitrogen matrix derived from infrared and Raman data: Comparison with argon matrix. *Journal of Raman Spectroscopy* **1981,** *11* (5), 406-415.
12. Brunel, L.-C.; Bureau, J.-C.; Peyron, M., Raman spectra of matrix isolated hydrogen and deuterium chloride: Monomers and dimers. *Chemical Physics* **1978,** *28* (3), 387-397.
13. West, W.; Arthur, P., The Raman spectra of some simple molecules in solution. *The Journal of Chemical Physics* **1937,** *5* (1), 10-13.
14. Li, L.; Zhang, X.; Luan, Z.; Du, Z.; Xi, S.; Wang, B.; Cao, L.; Lian, C.; Yan, J., Raman vibrational spectral characteristics and quantitative analysis of H2 up to 400° C and 40 MPa. *Journal of Raman Spectroscopy* **2018,** *49* (10), 1722-1731.
15. Cebeci-Maltaş, D.; Alam, M. A.; Wang, P.; Ben-Amotz, D., Photobleaching profile of Raman peaks and fluorescence background. *European Pharmaceutical Review* **2017,** *22* (6), 18-21.

APPENDIX A. ADDITIONAL FIGURES

APPENDIX A. ADDITIONAL FIGURES

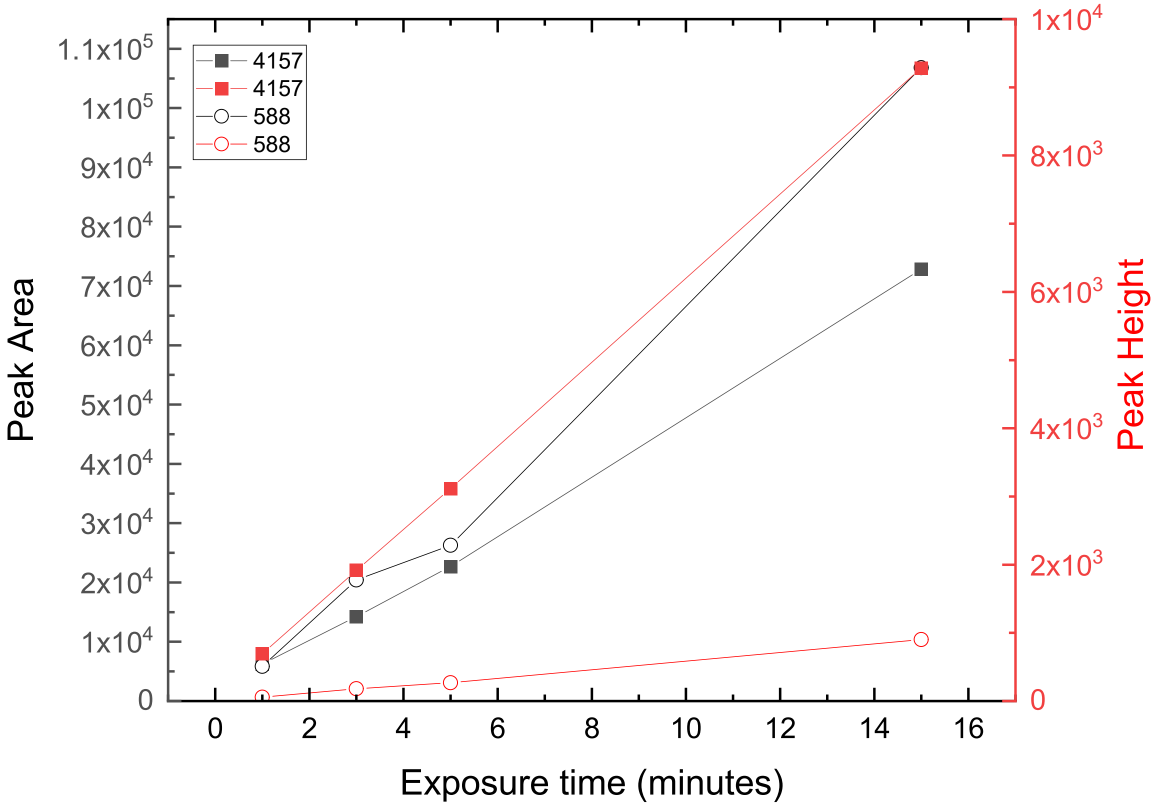

Figure A-1. Peak areas and heights of Raman spectra of 4% H_2(g) at 1.6 LPM from exposure times ranging from 1 to 5 min. In the key, 4157 and 588 refer to the wavelengths of the Raman peak (cm^{-1}) used to calculate area or height.

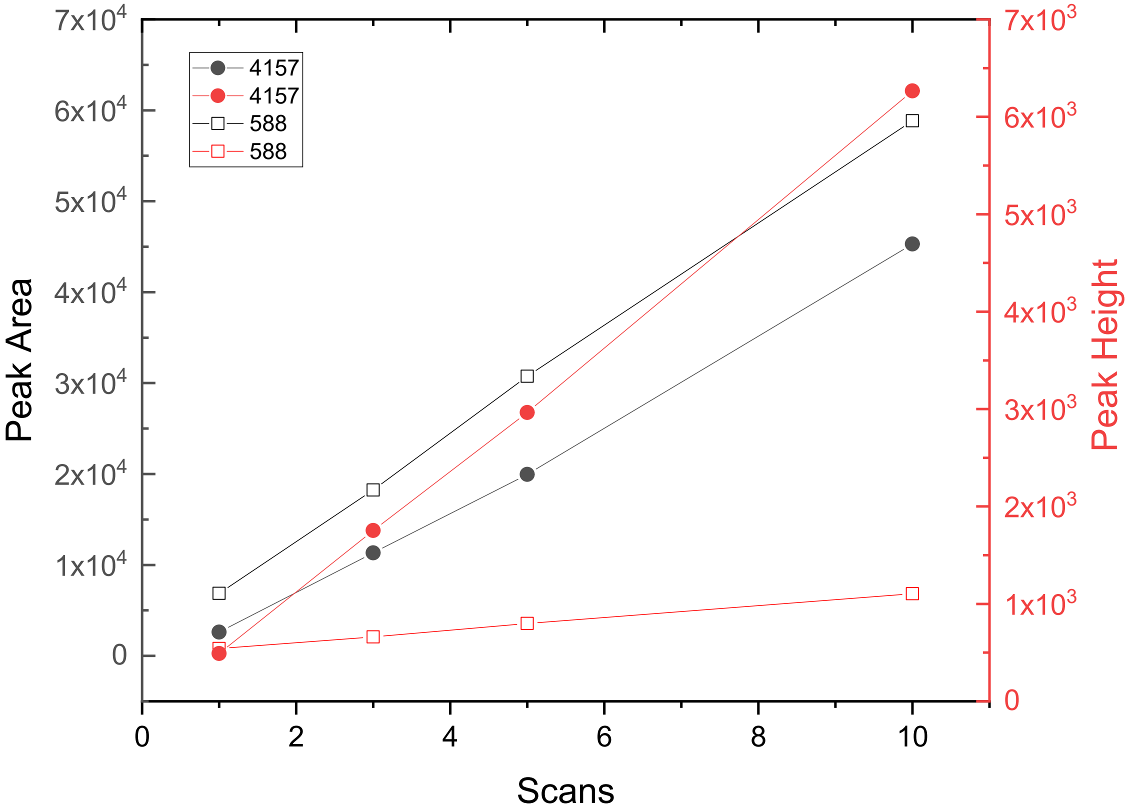

Figure A-2. Peak areas and heights of Raman spectra of 4% H_2(g) at 1.6 LPM from scan numbers ranging from 1 to 10. In the key, 4157 and 588 refer to the wavelengths of the Raman peak (cm^{-1}) used to calculate area or height.